Accepted Manuscript

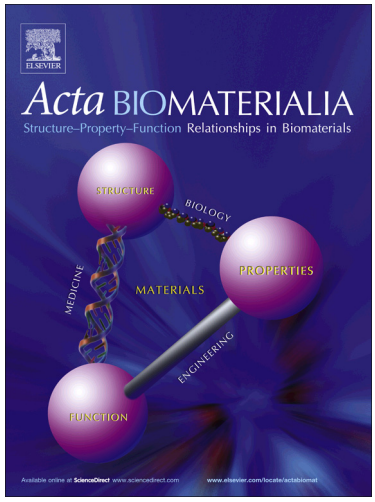

Full length article

Peptide and Peptide-Carbon Nanotube Hydrogels as Scaffolds for Tissue & 3D Tumor Engineering

Mohammadali Sheikholeslam, Scott D. Wheeler, Keely G. Duke, Mungo Marsden, Mark Pritzker, P. Chen

PII: S1742-7061(17)30768-7
DOI: https://doi.org/10.1016/j.actbio.2017.12.012
Reference: ACTBIO 5224

To appear in: *Acta Biomaterialia*

Received Date: 21 February 2016
Revised Date: 28 November 2017
Accepted Date: 8 December 2017

Please cite this article as: Sheikholeslam, M., Wheeler, S.D., Duke, K.G., Marsden, M., Pritzker, M., Chen, P., Peptide and Peptide-Carbon Nanotube Hydrogels as Scaffolds for Tissue & 3D Tumor Engineering, *Acta Biomaterialia* (2017), doi: https://doi.org/10.1016/j.actbio.2017.12.012

Peptide and Peptide-Carbon Nanotube Hydrogels as Scaffolds for Tissue & 3D Tumor Engineering

Mohammadali Sheikholeslam[1, 2], Scott D. Wheeler[2], Keely G. Duke[2], Mungo Marsden[3], Mark Pritzker[1] and P. Chen[1, 2,*]

[1]Department of Chemical Engineering, [2]Waterloo Institute for Nanotechnology, [3]Department of Biology, University of Waterloo, 200 University Avenue West, Waterloo, Ontario N2L 3G1, Canada

[*] Corresponding author. Tel: 519 888-4567 Ext. 31197. Email: p4chen@uwaterloo.ca (P. Chen)

ABSTRACT: The use of hybrid self-assembling peptide (EFK8)-carbon nanotube (SWNT) hydrogels for tissue engineering and *in vitro* 3D cancer spheroid formation is reported. These hybrid hydrogels are shown to enhance the attachment, spreading, proliferation and movement of NIH-3T3 cells relative to that observed using EFK8-only hydrogels. After five days, ~30% more cells are counted when the hydrogel contains SWNTs. Also, 3D encapsulation of these cells when injected in hydrogels does not adversely affect their behavior. Compressive modulus measurements and microscopic examination suggest that SWNTs have this beneficial effect by providing sites for cell anchorage, spreading and movement rather than by increasing hydrogel stiffness. This shows that the cells have a particular interaction with SWNTs not shared with EFK8 nanofibers despite a similar morphology. The effect of EFK8 and EFK8-SWNT hydrogels on A549 lung cancer cell behavior is also investigated. Increasing stiffness of EFK8-only hydrogels from about 44 Pa to 104 Pa promotes a change in A549 morphology from spheroidal to a stretched one similar to migratory phenotype. EFK8-SWNT hydrogels also promote a stretched morphology, but at lower stiffness. These results are discussed in terms of the roles of both microenvironment stiffness and cell-scaffold adhesion in cancer cell invasion. Overall, this study demonstrates that applications of peptide hydrogels *in vitro* can be expanded by incorporating SWNTs into their structure which further provides insight into cell-biomaterial interactions.

Keywords: self-assembling peptides, carbon nanotubes, hydrogels, tissue engineering, tumor microenvironment

1. Introduction

Hydrogels are commonly used biomaterials for tissue engineering and 3D cell cultures due to their high biocompatibility and the similarity of their physical and mechanical properties to that of living tissue [1]–[5]. These properties provide a compatible environment for cells and enable their behavior to be similar to that observed *in vivo*. Hydrogels can also be modified chemically to mimic living tissues so that they become more biocompatible and enhance their *in vivo* performance [1]–[3], [6].

Different types of materials have been used so far to make hydrogel scaffolds. Synthetic materials such as polylactic acid (PLA) [7], [8], polyethylene oxide (PEO) [9], polyglycolic acid (PGA) [10], polyvinyl alcohol (PVA) [11], [12], polyethylene glycol (PEG) [13], organosilica-based nanocomposites [14], [15] as well as polysaccharide hydrogels including hyaluronic acid (HA) [16], chitosan [17], agarose [18] and alginate [19] have been investigated for use with different types of tissues. Production of these synthetic polymers is reproducible which makes them attractive for researchers. However, hydrogels formed this way have major drawbacks such as large fiber/pore sizes, the use of toxic reagents for gel formation, low degradation under physiological conditions, improper charge density, low nutrient diffusion rate and acidic products due to degradation [20]. On the other hand, protein-based hydrogels using collagen [21], gelatin [22], fibrin [23], elastin [24], silk fibroin [25] and Matrigel™ are more biocompatible and biodegradable and provide a better platform for cell attachment and growth. However, they suffer from batch-to-batch variations and unwanted contaminants such as growth factors, proteins and viruses which can interfere with cell function [1], [20]. On the whole, the best option would be to use a synthetic material composed of naturally occurring components. Self-assembling peptides are very promising from this point of view. They are formed from

amino acids found ubiquitously in the body; at the same time, they can be synthesized with precise control of its chemical composition. This should minimize the effects of contaminants and enable the distinction between the effects of different cues on cell behavior in the prepared scaffold. Their biodegradation products are natural amino acids that are safe to cells and can be functionalized with different bioactive motifs for different cells and tissues. Also nano-sized fibers and pores of these hydrogels mimic the structure of living tissues *in vivo*. This provides an environment that can simulate *in-vivo* cell-cell and cell-scaffold interactions. In addition, fiber crosslinking by which hydrogels form from these peptides does not require any chemical additives, UV irradiation or heat treatment which can lead to lower cell biocompatibility, unlike the situation with other biopolymer-based hydrogels. Finally, these peptide hydrogels can be formed by injection which enables them to encapsulate cells for 3D cultures and be used *in vivo* with minimum need for surgery [26].

To date, different types of self-assembling peptide hydrogels have been used for biomedical applications ranging from hydrogels for tissue engineering [27][28] to nano-vehicles for anti-cancer drug and si-RNA delivery [29]. RADA16-I (RADARADARADARADA) hydrogels with the commercial name of PuraMatrix™ have been used as scaffolds in cell cultures [20]. The advantage of this peptide compared with other self-assembling peptides such as EFK8 (FEFEFKFK) is its similarity to the RGD (arginine-glycine-aspartic acid) tripeptide, a sequence within fibronectin that allows for cell attachment. Furthermore, the sequence of this peptide has been modified to extend its functionality and range of cells that can be seeded [30]. However, its mechanical strength drops after neutralization to the physiological pH which leads to its disruption when subjected to stress [31]. EFK8 is another type of self-assembling peptide with better mechanical strength due to stronger hydrophobic interactions conferred by the presence of phenylalanine [32]. Strong hydrophobic interactions, electrostatic and van der Waals' forces as

well as hydrogen bonding are the forces that drive EFK8 self-assembly. We have previously shown that EFK16-II and EFK8 peptides can disperse carbon nanotubes and be combined to form hybrid peptide-CNT hydrogels upon adding millimolar concentrations of monovalent salts [33], [34]. Although the suitability of CNTs and other carbon nanomaterials for biomedical applications is still an open question, many research studies have focused on their use in scaffolds for biomedical applications [35]–[51].

Another important application of hydrogels is for 3D cell cultures. Hydrogels have been used as 3D scaffolds for drug discovery and 3D cancer tumor studies *in vitro* [4], [5], [52]. A 3D environment changes the behavior (e.g. growth rate, morphology and drug resistance) of cultured cell lines compared to that of 2D environments, enabling cell behavior that more closely mimics that occurring *in vivo* [4], [53]–[56]. Both the extracellular matrix (ECM) and the physical properties of the microenvironment contribute significantly to the behavior and gene expression of cancer cells when they are *in vivo*. In contrast with the classical theory of cancer which posits accumulated gene mutations to be the main cause of cancer, tissue organization field theory (TOFT) introduces the cell-microenvironment interaction as the starting point for cancer [57][58]. It has even been reported that the placement of malignant tumor cells in a normal microenvironment can revert the cancer cells to a normal phenotype [59], [60]. With this approach, not only the tumor microenvironment can be a target for cancer therapy [61] but also bio-mimetic 3D scaffolds can serve as useful models of healthy ECM to treat the tumors *in vivo* and avoid the local formation of new tumors [52], [57], [62]. For these reasons, attention in recent years has been increasingly focused on the tumor microenvironment as an important controlling factor for cancer.

Although treatment of tumors through surgery, chemotherapy and radiation has progressed tremendously, the ability to accurately predict the metastatic potential of a tumor is still missing [63]. It has been well documented that tuning the scaffold stiffness can affect the growth and differentiation of different types of cells [64]–[69]. Stiffness has been shown to be an important characteristic of the microenvironment that affects tumor formation, progression and metastasis [70], [71]. Microenvironment stiffness can affect cell proliferation and differentiation so that the cells become metastatic [63], [72]–[74]. Thus, synthetic scaffolds with tunable compressive modulus can serve as useful artificial 3D microenvironments to study cancer cells, spheroids and tumors [75]–[79].

In the current work, we have investigated the effect of the presence of SWNTs in EFK8 hydrogels on the NIH-3T3 fibroblast cell adherence, proliferation, movement and spreading *in vitro* as well as the hydrogel compressive modulus. Also, the potential of EFK8 as a 3D scaffold with tunable compressive modulus to study A549 lung cancer cell spheroid formation *in vitro* has been examined. A549 cells were chosen due to similarity of the compressive modulus of the hydrogels to that of human lung tissue (< 1 kPa [80]). Finally, the effect of SWNT on the behavior of the cancer cells is investigated.

2. Materials and Methods

2.1 Materials

The ionic complementary peptide EFK8 with a sequence of FEFEFKFK was used in this study. This peptide was synthesized in our laboratory using an Aapptec Apex 396 peptide synthesizer Aapptec LLC (Louisville, KY, USA). The peptide was protected by acetyl and amino groups at the N terminus and C-terminus, respectively, to prevent end-to-end electrostatic interactions between peptides. In the peptide synthesis, cleavage was performed for 2h using the following

cleavage mixture: TFA (trifluoroacetic acid): TIS (Triisopropylsilane): water (95:2.5:2.5 volume ratio). Synthesis scale was based on one gram of resin and molar excess used during synthesis was 4. EFK8 was dissolved in pure water (18.2 M ; Millipore Milli-Q system) at a concentration of 2.5 mg ml^{-1} to prepare the peptide stock solution and then stored at 4°C before use. The metallic SWNTs (carbon > 90%, carbon as SWNT > 77%) were purchased from Sigma-Aldrich Co (catalog# 727777, lot# MKBH7136V). NIH-3T3 and A549 cells were purchased from ATCC. DMEM (high glucose) and F12-K medium solutions as well as fetal bovine serum (FBS) were obtained from HyClone™. Penicillin/streptomycin mixtures containing 10000 units penicillin and 10 mg streptomycin, Fluoroshield™ with DAPI and anti-β-catenin antibody produced from rabbits (C2206) were acquired from Sigma-Aldrich (Canada). Actin Green™ 488 ReadyProbes® reagent and Calcein AM (C3099) were purchased from Life Technologies. AffiniPure Donkey anti-Rabbit IgG (Jackson Immunoresearch laboratories Inc, West Grove, PA, USA) was used as the secondary antibody.

2.2 Methods

2.2.1 Peptide synthesis

All amino acids (Fmoc protected), activator 2-(6-chloro-1H-benzotriazole-1-yl)-1,1,3,3-tetramethylaminium hexafluorophosphate (HCTU) and Rink Amide-AM resin were obtained from Aapptec LLC. All other solutions were purchased from Acros Organics (NJ, USA). The EFK8 peptide with a molecular weight of 1162.60 g mol^{-1} was synthesized using the solid-phase peptide synthesis (SPPS) method using an Aapptec Apex 396 peptide synthesizer (Aapptec LLC, USA) and then purified by repeated precipitation in cold ether. The resulting peptide was then freeze-dried to yield a powder that was stored at 4°C. Matrix-assisted laser desorption ionization time-of-flight mass spectroscopy (MALDI-TOF MS) (Q-TOF Ultima Global, Waters, Milford,

MA, USA) was used to measure the molar mass of the synthesized peptide. Also high-performance liquid chromatography (HPLC) was employed to measure the purity of the peptide samples used in this study, which is found to be 72% (**Fig. S1**).

2.2.2 SWNT dispersion preparation

The stock suspensions were prepared by combining EFK8 and as-received SWNT (carbon > 90%, carbon as SWNT > 77%) together at a 1:1 mass ratio in pure water (18.2 M ; Millipore Milli-Q system) to yield concentrations of 0.5 mg ml^{-1} of both the peptide and SWNTs. Previous research in our laboratory has shown that the critical aggregation concentration of EFK8 in these EFK8-SWNT suspensions is below 0.1 mg/ml and these suspensions exhibit a zeta potential of ~ 56 mV [33]. The suspensions were then mixed for 1 hour using a Qsonica XL-2000 probe sonicator at a power of 10W and centrifuged at a speed of 2000 × g for 1h to separate the supernatant from the solids. Afterward, the supernatant was isolated for later use in hydrogel formation. It was also important to determine the EFK8 and SWNT concentration remaining in this supernatant since it was being used for hydrogel formation. To do this, we prepared 10 ml of the EFK8-SWNT suspension (with initial concentration of 0.5 mg/ml for both EFK8 and SWNT) and used a freeze-drying method to obtain dry material for thermogravimetric analysis (TGA). This involved freezing the dispersion for 24h at -80°C and then freeze-drying it for four days to remove the water content and leave behind a peptide-SWNT mixture. The composition of this freeze-dried mixture was then estimated by TGA over the temperature range from 25°C to 1000°C in a nitrogen atmosphere. As reported in a number of TGA analyses reported in the literature [81][82][83][84], peptides typically begin to thermally decompose at temperatures between 200°C and 300°C, and disappear completely before 600°C whereas SWNTs only begin to decompose at temperatures close to ~ 600°C. This behavior was supported by our TGA data

which showed a continuous mass loss beginning at 231°C up to 580°C (with a DTG peak at ~240.4°C) followed by a plateau in mass at temperatures between 580°C and ~ 648.5°C and then a resumption in mass loss above 648.5°C until the end of the experiment at 1000°C (**Fig. S2**). Based on this, we estimated the mass of EFK8 peptide and SWNT initially present in the freeze-dried peptide-SWNT mixture from the difference in the initial mass of the freeze-dried supernatant and the loss of mass as the sample was heated from 231°C to 580°C. From measurement of the weight loss, we determined that the EFK8 and SWNT concentration in the supernatant of a 0.5 mg/ml EFK8-SWNT dispersion was 0.12 mg/ml and 0.14 mg/ml respectively.

2.2.3 Hydrogel formation

Transparent PET membrane inserts with 1.0 μm pore size (BD Biosciences, San Jose, CA) were placed in 24-well cell culture plates. Then EFK8 and EFK8-SWNT solutions with the EFK8 concentration of 1.25 mg ml^{-1} were added to the inserts and cell culture medium was injected into the space between each insert and the well wall. Once monovalent salts present in the medium diffuse across the insert membrane, hydrogel formation was triggered through peptide charge screening by salt ions. The solutions were left exposed to UV light for 30 min at room temperature inside the biosafety hood to ensure sterilization of the hydrogel. To equilibrate the hydrogel with the medium, 400 μl of the cell culture medium was layered on top of the hydrogel and the plates transferred to a 37.0°C incubator. After an hour, two-thirds of the medium was gently removed and replaced with 400 μl of fresh medium before being placed in the 37.0°C incubator for another 1h. Finally, the medium in the insert was replaced and the medium in the well below the insert was replaced with 800 μl fresh medium and the plate was left in the incubator overnight.

2.2.4 Cell culture

Mouse NIH-3T3 fibroblast cells (12000 cells/well) were cultured on hydrogels formed in the 24-well inserts in the presence of Dulbecco's Modified Eagle's medium (DMEM, high glucose) with 10% fetal bovine serum and 1% penicillin/streptomycin (pH 7.4) and then transferred to an incubator containing 5% CO_2 at 37.0°C. Medium on top of the hydrogel and inside the wells was changed every 2-3 days. Human A549 lung cancer cells cultured in F12-K medium containing 10% FBS and 1% penicillin/streptomycin (pH 7.4) and maintained as described above.

2.2.5 Morphological and immunostaining

Calcein AM (8μM) was added to the cells and left for 30 min for morphological staining. To carry out staining, the medium was gently removed from the inserts and the cells were fixed in 4% paraformaldehyde for 20 minutes at room temperature, washed 3 times with PBS and the cells were permeabilized with 0.5 wt% Triton X-100 for 10 min. Then the hydrogels were washed three times with PBS. To reveal the actin cytoskeleton, one droplet of Actin Green™ probe was added to the hydrogel and left for 30 min followed by washing 3 times with PBS. Fluoroshield™ with DAPI was added to stain nuclei and left for 1 hour to penetrate into the hydrogel followed by 3 sequential washes of the surface with PBS. Also hydrogels were incubated in the blocking solution (PBS solution containing 10% fetal bovine serum) for 12-16 hours and fixed cells were stained for cell-cell junctions using anti- β-catenin (rabbit anti-β-catenin) at an anti- β-catenin antibody: blocking solution ratio of 1:500 and incubated at 4°C overnight. After washing the hydrogels with blocking solution four times (two hours per wash), the secondary antibody (donkey anti-rabbit IgG) was added to the blocking solution at a ratio of 1:250 and contents incubated for four hours. After three washes with PBS, the hydrogels were incubated in Fluoroshield™ with DAPI for 1h and washed three final times with PBS.

2.2.6 3D cell encapsulation

Stock EFK8 solution (5 mg ml^{-1}) was diluted 1:1 with sterile 20% w/v sucrose in H_2O. NIH-3T3 cells were washed 2 times in 10% w/v sucrose in H_2O, re-suspended in 10% sucrose to yield a density of 8×10^5 cell/well. The cell suspension was quickly mixed with an equal volume of the EFK8/10% sucrose solution to generate a final cell suspension (4×10^5 cell/ well) in EFK8 (1.25 mg ml^{-1}) and 10% sucrose. A 24-well plate was prepared with 250 µl of tissue culture medium/well. 100 µl of the cell suspension was added into each well insert. After five min, 400 µl tissue culture medium was gently layered over the gelled hydrogels. Plates were placed in the 37.0°C incubator and the medium was changed following the same procedure used to form the hydrogels (section 2.2.3). Experiments were repeated three times for each sample.

2.2.7 Microscopy

Images were taken using an EVOS fl digital inverted microscope (Life Technologies, USA) after 1, 3 and 5 days of incubation. For confocal imaging, the hydrogels were removed from the inserts and placed in chambered cover glasses facing (apical surface) down. PBS was added to prevent the hydrogels from drying during imaging. Confocal images were taken using a Zeiss LSM 510 Meta Confocal Microscope (Zeiss, Germany). The hydrogel samples were dried prior to SEM imaging by successive immersions in 30%, 50%, 70%, 90% and 100% ethanol solutions over a 2-day period. Once dehydrated, the hydrogels were prepared for microscopy using a custom-made critical point drier (CPD) employing supercritical CO_2. Scaffolds were fixed on aluminum stubs using carbon paste and gold sputtered for 100 sec prior to imaging using an FE-SEM (LEO 1530) unit. Again, experiments were repeated three times for each sample.

2.2.8 Micro-indentation

The compressive moduli of the hydrogels were measured using a micro-indenter equipped with a 0-25 g load cell (GSO-25, Transducer Techniques, CA, USA) and a hemispherical (D: 6mm) PDMS probe at a maximum load of 1g and speed of 5μ/s. Once again, experiments were repeated three times for each sample. The compressive modulus was calculated from the slope of the resulting stress-strain curve over the linear portion from 0 to 5% strain.

3. Results and Discussion

3.1 Effect of SWNT on cell attachment, spreading and proliferation

NIH-3T3 cells were seeded on the EFK8 hydrogel. **Figure 1a-c** show that NIH-3T3 cells that were initially spread over the surface of the EFK8 hydrogel tended to coalesce into colonies. As the colonies increase in size, the areas between them become almost free of cells. The cells that remain outside of the colonies display a rounded phenotype suggesting they adhere poorly to the hydrogel and form colonies due to the more favorable cell-cell adhesion over cell-hydrogel adhesion.

NIH 3T3 cells seeded on EFK8-SWNT hydrogels attach and spread more evenly across the hydrogel surface (Figure 1d-f). Most of the cells have a spindle-like morphology characteristic of NIH 3T3 cells. This demonstrates that the hybrid hydrogel provides a more suitable scaffold for the cells to attach and spread. Since the only difference between the hydrogels is the presence of SWNTs in the EFK8 scaffold, it is likely that this moiety provides sites that mediate cell attachment. This is in agreement with the previous reports on the effect of carbon-based nanomaterials such as CNTs and graphene on the cell behavior due to their strong affinity with the cells and specially as a result of their aromatic structure which can increase the local concentration of ECM proteins such as collagen, laminin and fibronectin [85][86]. We have previously shown that when EFK8 peptides interact with SWNTs, they tend to wrap around them

with a helical pattern [34]. This helical pattern should still leave some portions of SWNT accessible for the cells to reach. Although not included here, we found that the cells did not exhibit any change in behavior when the SWNT concentration used to generate the hydrogels was decreased four-fold. Although CNTs have been found to enhance cell attachment, proliferation and differentiation, the mechanism by which they interact with cells has not been investigated and is beyond the scope of this study. Nevertheless, it is worth noting that the gelation of these self-assembling peptides is driven by neutralization of their electrostatic charge promoted by monovalent salt ions present in the cell culture medium. Thus, we would expect the overall charge of both the EFK8 and EFK8-SWNT hydrogels to be zero [87][88]. Thus, the differences in the cell behavior in the presence of these two hydrogels cannot be correlated to differences in hydrogel charge. The confocal microscopy images in Figure 1g and h show NIH 3T3 cells after 3 days incubation on EFK8 and EFK8-SWNT hydrogel, respectively. In these higher magnification images, the difference in the cells in these two environments is more obvious. The cells on EFK8 clearly form clusters with actin accumulating along the cell boundaries, while they are more spread out on EFK8-SWNT and actin is arranged in stress fibers indicative of strong substrate adhesion.

Also Figure1i shows cells seeded on RADA16-I hydrogel as a control sample. The resulting image shows that the hydrogel is disrupted after one day and cannot maintain its initial shape which can hinder its application for transplanting *in-vivo*, although the cells can attach and proliferate very well with a spindle-like morphology on the RADA16-I hydrogel (due to similarity of the peptide sequence to RGD), in agreement with that reported in the literature [31].

Figure 2 presents SEM images of fixed cells on the hydrogels. These images show that cells move on the EFK8 hydrogel to form small clusters (Figure 2a). From the higher magnification

image in Figure 2b, the aggregation of cells into small colonies is very apparent. On the other hand, when cells are seeded on the EFK8-SWNT hydrogel, they remain dispersed and display a classic spindle-shaped morphology (Fig 2c). Higher magnification images of an individual cell on the hybrid EFK8-SWNT hydrogel are shown in Figure 2c-f. Cells display both lamellipodia (Figure 2d, e) as well as numerous filopodia (Fig 2e, f), indicative of their strong adhesion to the hybrid hydrogel.

The different cell behavior shown in Figure 1 suggests that cells proliferate faster on the EFK8-SWNT hydrogel and more cells are living in this scaffold after 5 days. To compare the proliferation rate of cells seeded on the two hydrogels, the gels were disrupted and the cells collected and mixed with trypan blue. Live cells were counted using a hemocytometer after 1, 3 and 5 days of culture (**Figure 3a**). The cell viability was found to be more than 90% in all samples except for EFK8 at day one which may be due to the higher number of non-attached cells on the hydrogel that have died (Figure 3b). However this analysis shows that the number of cells is similar on both hydrogels one day after seeding. But, over the period from day one to day three after seeding, cells proliferate at a higher rate on the hybrid hydrogel. The difference in the proliferation rate of cells continues to diverge over the period from day three to day five (Figure 3a).

Thus, based on these microscopy images and cell counting data, the presence of SWNTs in the EFK8 hydrogel appears to alter cell behavior so that cell attachment, spreading and proliferation rate is enhanced.

3.2 Effect of SWNT on cell movement

To better investigate cell movement in the two types of hydrogels, a small droplet of EFK8-SWNT dispersion was placed on the EFK8 solution and then gelation was triggered simultaneously in both of the hydrogels. In this way, isolated hybrid EFK8-SWNT hydrogels were distributed over the surface of the EFK8 hydrogel. The sample was then examined using light and confocal microscopy. **Figure 4a** is a transmitted light image showing stretched cells populating an isolated EFK8-SWNT hydrogel surrounded by cell colonies on the EFK8 hydrogel three days after seeding cells. This clearly shows the contrast between the stretched morphology that cells can assume in the hybrid hydrogel and the rounded shapes in the colonies that form when the hydrogel consists of EFK8 alone. A confocal image of the same region better highlights the difference in cell morphology on the two portions of the surface (Figure 4b). Three-dimensional reconstruction of confocal images clearly demonstrates the difference in the adhesive properties of the two hydrogels. Figure 4c and d show reconstructed 3-dimensional images of these cells at two different angles. Although cells were originally seeded only on the very top of the hydrogel, cells appear to have penetrated vertically into the hydrogel. This effect further depicts the role of CNT in improving cell-scaffold interactions and enhancing cell movement.

3.3 3D encapsulation of cells inside hydrogels

One of the major applications of hydrogels in tissue engineering is to encapsulate and deliver cells to a desired target *in-vivo*. Typically, the hydrogel is transplanted into the injured area after surgery to gain access. However, an advantage of injectable hydrogels is the minimal wound produced during cell transplantation. To do so, cells should be already encapsulated in the hydrogel precursor dispersion prior to injection. To test this idea, cells were dispersed in EFK8 and EFK8-SWNT dispersions and hydrogels formed. **Figure 5** presents optical images of cells in

EFK8 and EFK8-SWNT hydrogels after one, three and five days of encapsulation. As can be seen, cells show similar behavior to that observed previously when they were seeded on top of a pre-existing EFK8 and hybrid hydrogel (Figure 1). In the EFK8 hydrogel, cells stretch and move toward each other to form colonies over the period from day one to day five (Figure 5a-c). Once again, this result indicates that cells cannot anchor and adhere very well to the scaffold in this hydrogel and show the natural morphology of fibroblast cells. The images obtained on the hybrid hydrogel (Figure 5d-f) show that no significant difference between cell morphologies is observed in the two types of hydrogels on day one. However, the behavior changes thereafter as the cells exhibit stretched morphology and spread well inside the hybrid hydrogel by days three and five. These results also demonstrate that embedding NIH-3T3 cells in the EFK8-SWNT hydrogel has no adverse effect on cell viability and behavior.

3.4 Compressive modulus of hydrogels

The compressive moduli of EFK8 hydrogels formed at different peptide concentrations as well as the hybrid EFK8-SWNT hydrogel are presented in **Figure 6a**. As can be seen, an increase in the peptide concentration raises the modulus of the EFK8 hydrogel. Also, a comparison of results obtained for the EFK8 and EFK8-SWNT hydrogels formed from the same peptide concentration of 1.25 mg ml^{-1} shows that the presence of SWNT in the EFK8 hydrogel does not significantly change its modulus. This can be attributed to the very low concentration of SWNTs in the hydrogel. Thus, the previously noted difference in the cell behavior on these two hydrogels is not likely caused by a change in the stiffness, as has been reported in some previous studies [64]–[69]. This trend supports the conclusion that the difference is due to the ability of SWNT itself to provide appropriate sites for cell anchorage. This result is further confirmed by observation of the behavior of NIH-3T3 cells cultured on a stiffer EFK8 hydrogel formed from a peptide

concentration of 5 mg ml^{-1}. On the other hand considering similar morphology of peptide nanofibers and SWNTs in the hydrogel reveals that the cells have a particular interaction with SWNTs which is not shared with EFK8 nanofibers. The image of these cells taken after five days and shown in Figure 6b does not show any distinctive difference in the cell morphology on this hydrogel and the less stiff EFK8 hydrogel formed from 1.25 mg ml^{-1} previously presented in Figure 1c. The cells form colonies even on this stiffer hydrogel, whereas the cell morphology is very different when cultured on the hybrid EFK8-SWNT hydrogel.

3.5 EFK8 and EFK8-SWNT hydrogels as scaffolds for engineering cancer cell spheroids

In the final stage of this study, A549 lung cancer cells were seeded on the hydrogels to evaluate the suitability of EFK8 and EFK8-SWNT hydrogels as 3D cell culture platforms to study the formation of spheroidal cancer cells. As can be seen in **Figure 7** (left column), cancer cells grow over time and form spheroidal colonies on an EFK8 hydrogel. Furthermore, these tumor-like spheroids grow over time on the hydrogel. This shows that an EFK8 hydrogel can be used as a 3D cell culture platform triggering cancer cells to form spheroids which is more similar to the morphology of real tumors than that obtained with 2D cell cultures.

To explore whether the compressive modulus of the hydrogel has any effect on the behavior of the cancer spheroids, A459 cells were seeded on a stiffer EFK8 hydrogel formed from 5 mg ml^{-1} peptide solution. The optical images shown in Figure 7 (middle column) indicate that increasing the compressive modulus from about 44 Pa to 104 Pa leads to more stretched cells with a higher potential for spreading and movement, demonstrating the role of microenvironment stiffness in cancer cell invasion. This contrasts with the NIH-3T3 cell behavior on the stiffer hydrogel that shows no dependence on change in hydrogel compressive modulus. This reflects that the threshold of sensitivity to scaffold stiffness may vary from cell to cell. Interestingly, as shown in

the right column of Figure 7, the addition of SWNTs to the EFK8 hydrogel formed from 1.25 mg ml^{-1} peptide leads to similar cell morphology (stretched cells with long protrusions) to that observed on EFK8 alone when formed from 5 mg ml^{-1} peptide. Earlier in this study, we showed that the presence of SWNTs in an EFK8 hydrogel improved normal cell attachment, spreading and movement. Thus, the behavior of A549 cells when seeded on EFK8-SWNT likely reflects the effect that binding regions in the tumor microenvironment and cell-biomaterial interaction (in addition to that of compressive modulus) have on cancer metastasis.

Figure 8a, b shows cells that have been stained using the Calcein AM on EFK8 hydrogels formed from both 1.25 and 5 mg ml^{-1} peptide. In Figure 8a the green color of Calcein AM is replaced with a spectrum of different colors that represent different distances from the hydrogel surface to better reflect the 3D character of the spheroids. These images show that the cells have spheroidal geometry when grown on the hydrogel formed at 1.25 mg ml^{-1} peptide (Figure 8a) and stretched morphology when grown on the hydrogel formed at the higher peptide concentration (Figure 8b). Immunostaining for -catenin, which is normally concentrated at the cell-cell junctions, and of the cell nucleus using DAPI was also conducted. Figure 8c shows that cells seeded on the EFK8 hydrogel formed from 1.25 mg ml^{-1} peptide form spheroids that pack together with sharp polygonal boundaries, characteristic of compact cells in colonies, and have concentrated green -catenin color on the edges. In the case of the EFK8 hydrogel formed from 5 mg ml^{-1} peptide (Figure 8d) and the EFK8-SWNT hydrogel (Figure 8e), although similar polygonal boundaries can be seen in some parts (specially on the first hydrogel), but some cells at the border of the spheroids have stretched morphology, contain less concentrated -catenin on the edges and do not have sharp polygonal boundary. This suggests that these cells are not strongly attached to their neighbor cells which should facilitate colony dissociation and

individual cell movement. This is apparent from the morphology of some of the cells especially on the hybrid hydrogel.

4. Conclusions

It was shown that the presence of SWNTs in the EFK8 hydrogel significantly increases NIH-3T3 cell attachment and leads to a spindle-like morphology, an indication of healthy cells. Also, cells proliferate faster on the SWNT-containing hydrogel. It was observed that cells spread evenly and move more on the hybrid hydrogel than on an EFK8 hydrogel, both in 2D and 3D cultures. This contrast in cell behavior may be useful for cell patterning in future work. Furthermore, EFK8-SWNT is able to encapsulate the cells for use in delivery applications, while the presence of SWNTs in the hydrogel did not hinder the cell behavior observed in 2D cultures. An increase of the peptide concentration was found to raise the compressive modulus of the resulting hydrogels. However, the presence of the SWNT in the EFK8 hydrogel did not have an effect on its compressive modulus. Also, culturing the cells on a stiffer hydrogel made no significant difference to the apparent behavior of NIH-3T3 cells. Thus, we conclude that the improvement in NIH-3T3 cell attachment, growth, spreading and movement on the hybrid hydrogel is not related to the change in modulus and instead is probably related to the enhanced cell-scaffold attachment. Considering similar morphology of peptide fibers and SWNTs in the hydrogel, this shows that SWNTs have a particular interaction with the cells which is not shared by the EFK8 nanofibers. EFK8 hydrogels can also be used as 3D cell culture scaffolds for cancer cells. They were found to promote formation of A549 cancer cell spheroids which grow by time and can be used for 3D drug screening. In contrast with the NIH-3T3 cell behavior, an increase in the compressive modulus of the hydrogel leads to A549 cells with a more stretched morphology and able to move more easily over the surface, demonstrating the role of microenvironment stiffness

in cancer cell invasion. This also shows that different cells may have different thresholds of sensitivity to the scaffold stiffness. On the other hand, the addition of SWNTs to the EFK8 hydrogel (while keeping its modulus unchanged) results in cells with mobility similar to that observed on stiffer hydrogels, signifying the importance of cell-scaffold interactions to metastasis. Finally this study demonstrates that incorporating SWNTs into peptide hydrogels can expand applications of these hydrogels in tissue engineering and can give further insight into cell-biomaterial interactions.

Acknowledgments

The authors appreciate funding from the Natural Sciences and Engineering Research Council of Canada (NSERC) and the Canada Foundation for Innovation (CFI) to carry out this research. In addition, support from the Canada Research Chairs (CRC) program for one of the coauthors (P.C.) is gratefully acknowledged. Also we appreciate Dr. Adrienne Boone for her helps in imaging by confocal microscopy.

5. References

[1] K. Y. Lee and D. J. Mooney, “Hydrogels for Tissue Engineering,” *Chem. Rev.*, vol. 101, no. 7, pp. 1869–1880, Jul. 2001.

[2] J. L. Drury and D. J. Mooney, “Hydrogels for tissue engineering: scaffold design variables and applications,” *Biomaterials*, vol. 24, no. 24, pp. 4337–4351, Nov. 2003.

[3] Y. Li, J. Rodrigues, and H. Tomás, “Injectable and biodegradable hydrogels: gelation, biodegradation and biomedical applications.,” *Chem. Soc. Rev.*, vol. 41, no. 6, pp. 2193–221, Mar. 2012.

[4] L. A. Gurski, N. J. Petrelli, X. Jia, and M. C. Farach-Carson, “3D Matrices for Anti-

Cancer Drug Testing and Development," *Oncol. Issues*, no. January/ February, pp. 20–25, 2010.

[5] S. Breslin and L. O. Driscoll, "Three-dimensional cell culture: the missing link in drug discovery," *Drug Discov. Today*, vol. 18, no. 5/6, pp. 240–249, 2013.

[6] F. Brandl, F. Sommer, and A. Goepferich, "Rational design of hydrogels for tissue engineering: impact of physical factors on cell behavior.," *Biomaterials*, vol. 28, no. 2, pp. 134–46, Jan. 2007.

[7] D. A. Barrera, E. Zylstra, P. T. Lansbury, and R. Langer, "Synthesis and RGD peptide modification of a new biodegradable copolymer: poly(lactic acid-co-lysine)," *J. Am. Chem. Soc*, vol. 115, no. 23, pp. 11010–11011, 1993.

[8] A. J. R. Lasprilla, G. a R. Martinez, B. H. Lunelli, A. L. Jardini, and R. M. Filho, "Poly-lactic acid synthesis for application in biomedical devices - a review.," *Biotechnol. Adv.*, vol. 30, no. 1, pp. 321–8, 2012.

[9] J. Elisseeff, W. Mcintosh, K. Anseth, S. Riley, P. Ragan, and R. Langer, "Photoencapsulation of chondrocytes in poly (ethylene oxide)-based semi-interpenetrating networks," *J Biomed Mater Res*, vol. 51, no. 2, pp. 164–171, 2000.

[10] D. J. Mooney, C. L. Mazzoni, C. Breued, K. Mcnamara, D. Hem, J. P. Vacanti, and R. Langer, "Stabilized polyglycolic acid fibre-based tubes for tissue engineering," *Biomaterials*, vol. 17, no. 2, pp. 115–124, 1996.

[11] R. H. Schmedlen, K. S. Masters, and J. L. West, "Photocrosslinkable polyvinyl alcohol hydrogels that can be modified with cell adhesion peptides for use in tissue engineering," *Biomaterials*, vol. 23, pp. 4325–4332, 2002.

[12] M. I. Baker, S. P. Walsh, Z. Schwartz, and B. D. Boyan, "A review of polyvinyl alcohol and its uses in cartilage and orthopedic applications.," *J. Biomed. Mater. Res. B. Appl. Biomater.*, vol. 100, no. 5, pp. 1451–7, Jul. 2012.

[13] J. Zhu, "Bioactive modification of poly(ethylene glycol) hydrogels for tissue engineering.," *Biomaterials*, vol. 31, no. 17, pp. 4639–56, Jun. 2010.

[14] N. S. Kehr, E. A. Prasetyanto, K. Benson, B. Ergün, A. Galstyan, and H. J. Galla, "Periodic mesoporous organosilica-based nanocomposite hydrogels as three-dimensional scaffolds," *Angew. Chemie - Int. Ed.*, vol. 52, no. 4, pp. 1156–1160, 2013.

[15] N. Seda Kehr and K. Riehemann, "Controlled Cell Growth and Cell Migration in Periodic Mesoporous Organosilica/Alginate Nanocomposite Hydrogels," *Adv. Healthc. Mater.*, vol. 5, pp. 193–197, 2016.

[16] M. N. Collins and C. Birkinshaw, "Hyaluronic acid based scaffolds for tissue engineering--a review.," *Carbohydr. Polym.*, vol. 92, no. 2, pp. 1262–79, Feb. 2013.

[17] F. Croisier and C. Jérôme, "Chitosan-based biomaterials for tissue engineering," *Eur. Polym. J.*, vol. 49, no. 4, pp. 780–792, Apr. 2013.

[18] T. Gros, J. S. Sakamoto, A. Blesch, L. A. Havton, and M. H. Tuszynski, "Regeneration of long-tract axons through sites of spinal cord injury using templated agarose scaffolds.," *Biomaterials*, vol. 31, no. 26, pp. 6719–29, Sep. 2010.

[19] K. Y. Lee and D. J. Mooney, "Alginate: properties and biomedical applications," *Prog. Polym. Sci.*, vol. 37, no. 1, pp. 106–126, Jan. 2012.

[20] S. Zhang, X. Zhao, and L. Spirio, "PuraMatrix: self-assembling peptide nanofiber scaffolds," in *Scaffolding in tissue engineering*, P. X. . Ma and J. Elisseeff, Eds. CRC

Press, 2005, pp. 217–238.

[21] J. Glowacki and S. Mizuno, "Collagen scaffolds for tissue engineering.," *Biopolymers*, vol. 89, no. 5, pp. 338–44, May 2008.

[22] S.-M. Lien, L.-Y. Ko, and T.-J. Huang, "Effect of pore size on ECM secretion and cell growth in gelatin scaffold for articular cartilage tissue engineering.," *Acta Biomater.*, vol. 5, no. 2, pp. 670–9, Feb. 2009.

[23] T. A. E. Ahmed, E. V Dare, and M. Hincke, "Fibrin: a versatile scaffold for tissue engineering applications.," *Tissue Eng. Part B. Rev.*, vol. 14, no. 2, pp. 199–215, Jun. 2008.

[24] W. Daamen, J. Veerkamp, J. Vanhest, and T. Vankuppevelt, "Elastin as a biomaterial for tissue engineering," *Biomaterials*, vol. 28, no. 30, pp. 4378–4398, Oct. 2007.

[25] C. Vepari and D. L. Kaplan, "Silk as a Biomaterial.," *Prog. Polym. Sci.*, vol. 32, no. 8–9, pp. 991–1007, Jan. 2007.

[26] E. C. Wu, S. Zhang, and C. A. E. Hauser, "Self-Assembling Peptides as Cell-Interactive Scaffolds," *Adv. Funct. Mater.*, vol. 22, no. 3, pp. 456–468, Feb. 2012.

[27] Y. Loo, S. Zhang, and C. A. E. Hauser, "From short peptides to nanofibers to macromolecular assemblies in biomedicine.," *Biotechnol. Adv.*, vol. 30, no. 3, pp. 593–603, 2012.

[28] S. Kim, J. H. Kim, J. S. Lee, and C. B. Park, "Beta-sheet-forming, self-assembled peptide nanomaterials towards optical, energy, and healthcare applications," *Small*, vol. 11, no. 30, pp. 3623–3640, 2015.

[29] S. Y. Fung, H. Yang, P. T. Bhola, P. Sadatmousavi, E. Muzar, M. Liu, and P. Chen, "Self-

Assembling Peptide as a Potential Carrier for Hydrophobic Anticancer Drug Ellipticine: Complexation, Release and In Vitro Delivery," *Adv. Funct. Mater.*, vol. 19, no. 1, pp. 74–83, Jan. 2009.

[30] Y. Loo, S. Zhang, and C. A. E. Hauser, "From short peptides to nanofibers to macromolecular assemblies in biomedicine," *Biotechnol. Adv.*, vol. 30, no. 3, pp. 593–603, 2012.

[31] Y. Nagai, H. Yokoi, K. Kaihara, and K. Naruse, "The mechanical stimulation of cells in 3D culture within a self-assembling peptide hydrogel.," *Biomaterials*, vol. 33, no. 4, pp. 1044–51, Feb. 2012.

[32] R. T. Lee, R. D. Kamm, D. Narmoneva, and S. Zhang, "Angiogenesis and Cardiac Tissue Engineering with Peptide Hydrogels and Related Compositions and Methods of Use Thereof," 2003.

[33] M. Sheikholeslam, M. Pritzker, and P. Chen, "Dispersion of multiwalled carbon nanotubes in water using ionic-complementary peptides.," *Langmuir*, vol. 28, no. 34, pp. 12550–6, Aug. 2012.

[34] M. Sheikholeslam, M. Pritzker, and P. Chen, "Hybrid peptide–carbon nanotube dispersions and hydrogels," *Carbon N. Y.*, vol. 71, pp. 284–293, May 2014.

[35] N. S. Satarkar, D. Johnson, B. Marrs, R. Andrews, C. Poh, B. Gharaibeh, K. Saito, K. W. Anderson, and J. Z. Hilt, "Hydrogel-MWCNT Nanocomposites•: Synthesis , Characterization , and Heating with Radiofrequency Fields," *J. ofAppliedPolymer Sci.*, vol. 117, pp. 1813–1819, 2010.

[36] B. Adhikari and A. Banerjee, "Short peptide based hydrogels: incorporation of graphene into the hydrogel," *Soft Matter*, vol. 7, no. 19, p. 9259, 2011.

[37] X. Meng, D. A. Stout, L. Sun, R. L. Beingessner, H. Fenniri, and T. J. Webster, "Novel injectable biomimetic hydrogels with carbon nanofibers and self assembled rosette nanotubes for myocardial applications.," *J. Biomed. Mater. Res. A*, pp. 1–8, Sep. 2012.

[38] S. R. Shin, H. Bae, J. M. Cha, J. Y. Mun, Y.-C. Chen, H. Tekin, H. Shin, S. Farshchi, M. R. Dokmeci, S. Tang, and A. Khademhosseini, "Carbon nanotube reinforced hybrid microgels as scaffold materials for cell encapsulation.," *ACS Nano*, vol. 6, no. 1, pp. 362–72, Jan. 2012.

[39] W. H. Marks, S. C. Yang, G. W. Dombi, and S. K. Bhatia, "Translational potential for hydrogel composites containing carbon nanobrushes," in *38th Annual Northeast Bioengineering Conference (NEBEC)*, 2012, pp. 392–393.

[40] E. Soliman, S. C. Yang, G. W. Dombi, and S. K. Bhatia, "Electrically Conductive , Biocompatible Composite Containing Carbon Nanobrushes for Applications in Neuroregeneration," in *38th Annual Northeast Bioengineering Conference (NEBEC)*, 2012, pp. 343–344.

[41] S. R. Shin, S. M. Jung, M. Zalabany, K. Kim, P. Zorlutuna, S. Kim, M. Nikkhah, M. Khabiry, M. Azize, J. Kong, K. Wan, T. Palacios, M. R. Dokmeci, H. Bae, X. (Shirley) Tang, and A. Khademhosseini, "Carbon-Nanotube-Embedded Hydrogel Sheets for Engineering Cardiac Constructs and Bioactuators," *ACS Nano*, vol. 7, no. 3, pp. 2369–2380, 2013.

[42] E. Cheng, Y. Li, Z. Yang, Z. Deng, and D. Liu, "DNA-SWNT hybrid hydrogel.," *Chem. Commun. (Camb).*, vol. 47, no. 19, pp. 5545–7, May 2011.

[43] R. A. MacDonald, B. F. Laurenzi, G. Viswanathan, P. M. Ajayan, and J. P. Stegemann, "Collagen-carbon nanotube composite materials as scaffolds in tissue engineering.," *J.*

Biomed. Mater. Res. A, vol. 74, no. 3, pp. 489–96, Sep. 2005.

[44] R. A. MacDonald, C. M. Voge, M. Kariolis, and J. P. Stegemann, "Carbon nanotubes increase the electrical conductivity of fibroblast-seeded collagen hydrogels.," *Acta Biomater.*, vol. 4, no. 6, pp. 1583–92, Nov. 2008.

[45] C. M. Homenick, H. Sheardown, and A. Adronov, "Reinforcement of collagen with covalently-functionalized single-walled carbon nanotube crosslinkers," *J. Mater. Chem.*, vol. 20, no. 14, p. 2887, 2010.

[46] Z. Tosun and P. S. McFetridge, "A composite SWNT-collagen matrix: characterization and preliminary assessment as a conductive peripheral nerve regeneration matrix.," *J. Neural Eng.*, vol. 7, no. 6, p. 66002, Dec. 2010.

[47] Y. Cho and R. Ben Borgens, "The effect of an electrically conductive carbon nanotube/collagen composite on neurite outgrowth of PC12 cells.," *J. Biomed. Mater. Res. A*, vol. 95, no. 2, pp. 510–7, Nov. 2010.

[48] W. Tan, J. Twomey, D. Guo, K. Madhavan, and M. Li, "Evaluation of nanostructural, mechanical, and biological properties of collagen-nanotube composites.," *IEEE Trans. Nanobioscience*, vol. 9, no. 2, pp. 111–20, Jun. 2010.

[49] B. L. Behan, D. G. DeWitt, D. R. Bogdanowicz, A. N. Koppes, S. S. Bale, and D. M. Thompson, "Single-walled carbon nanotubes alter Schwann cell behavior differentially within 2D and 3D environments.," *J. Biomed. Mater. Res. A*, vol. 96, no. 1, pp. 46–57, Jan. 2011.

[50] C. M. Voge, J. Johns, M. Raghavan, M. D. Morris, and J. P. Stegemann, "Wrapping and dispersion of multiwalled carbon nanotubes improves electrical conductivity of protein-nanotube composite biomaterials.," *J. Biomed. Mater. Res. A*, pp. 1–8, Aug. 2012.

[51] J. Y. Lee, C. A. Bashur, C. A. Milroy, L. Forciniti, A. S. Goldstein, and C. E. Schmidt, "Nerve growth factor-immobilized electrically conducting fibrous scaffolds for potential use in neural engineering applications.," *IEEE Trans. Nanobioscience*, vol. 11, no. 1, pp. 15–21, Mar. 2012.

[52] C. Fischbach, R. Chen, T. Matsumoto, T. Schmelzle, J. S. Brugge, P. J. Polverini, and D. J. Mooney, "Engineering tumors with 3D scaffolds," *Nat. Methods*, vol. 4, no. 10, pp. 855–860, 2007.

[53] L. A. Gurski, A. K. Jha, C. Zhang, X. Jia, and M. C. Farach-Carson, "Hyaluronic acid-based hydrogels as 3D matrices for in vitro evaluation of chemotherapeutic drugs using poorly adherent prostate cancer cells.," *Biomaterials*, vol. 30, no. 30, pp. 6076–85, Oct. 2009.

[54] C. Feder-Mengus, S. Ghosh, A. Reschner, I. Martin, and G. C. Spagnoli, "New dimensions in tumor immunology: what does 3D culture reveal?," *Trends Mol. Med.*, vol. 14, no. 8, pp. 333–40, Aug. 2008.

[55] L. David, V. Dulong, D. Le Cerf, L. Cazin, M. Lamacz, and J.-P. Vannier, "Hyaluronan hydrogel: an appropriate three-dimensional model for evaluation of anticancer drug sensitivity.," *Acta Biomater.*, vol. 4, no. 2, pp. 256–63, Mar. 2008.

[56] J. L. Horning, S. K. Sahoo, S. Vijayaraghavalu, S. Dimitrijevic, J. K. Vasir, T. K. Jain, A. K. Panda, and V. Labhasetwar, "3-D Tumor Model for In Vitro Evaluation of Anticancer Drugs," *Mol. Pharm.*, vol. 5, no. 5, pp. 849–862, 2008.

[57] M. Bizzarri, A. Cucina, and S. Proietti, "The tumor microenvironment as a target for anticancer treatment," *Oncobiology and Targets*, vol. 1, no. 1, pp. 3–11, 2014.

[58] A. M. Soto and C. Sonnenschein, "The tissue organization field theory of cancer: a

testable replacement for the somatic mutation theory.," *Bioessays*, vol. 33, no. 5, pp. 332–40, May 2011.

[59] P. A. Kenny and M. J. Bissell, "Tumor reversion: correction of malignant behavior by microenvironmental cues.," *Int. J. Cancer*, vol. 107, no. 5, pp. 688–95, Dec. 2003.

[60] M. J. C. Hendrix, E. A. Seftor, R. E. B. Seftor, J. Kasemeier-Kulesa, P. M. Kulesa, and L.-M. Postovit, "Reprogramming metastatic tumour cells with embryonic microenvironments.," *Nat. Rev. Cancer*, vol. 7, no. 4, pp. 246–55, Apr. 2007.

[61] A. Albini and M. B. Sporn, "The tumour microenvironment as a target for chemoprevention," *Nat. Rev. Cancer*, vol. 7, no. 2, pp. 139–147, Feb. 2007.

[62] E. Hanna, J. Quick, and S. K. Libutti, "The tumour microenvironment: a novel target for cancer therapy," *Oral Dis.*, vol. 15, no. 1, pp. 8–17, Jan. 2009.

[63] C. M. Kraning-Rush, J. P. Califano, and C. A. Reinhart-King, "Cellular traction stresses increase with increasing metastatic potential.," *PLoS One*, vol. 7, no. 2, p. e32572, Jan. 2012.

[64] J. B. Leach, X. Q. Brown, J. G. Jacot, P. A. Dimilla, and J. Y. Wong, "Neurite outgrowth and branching of PC12 cells on very soft substrates sharply decreases below a threshold of substrate rigidity.," *J. Neural Eng.*, vol. 4, no. 2, pp. 26–34, Jun. 2007.

[65] K. Saha, A. J. Keung, E. F. Irwin, Y. Li, L. Little, D. V Schaffer, and K. E. Healy, "Substrate modulus directs neural stem cell behavior.," *Biophys. J.*, vol. 95, no. 9, pp. 4426–38, Nov. 2008.

[66] N. D. Leipzig and M. S. Shoichet, "The effect of substrate stiffness on adult neural stem cell behavior.," *Biomaterials*, vol. 30, no. 36, pp. 6867–78, Dec. 2009.

[67] M. T. Frey and Y.-L. Wang, "A photo-modulatable material for probing cellular responses to substrate rigidity.," *Soft Matter*, vol. 5, pp. 1918–1924, Jan. 2009.

[68] P. A. Galie, M. V Westfall, and J. P. Stegemann, "Reduced serum content and increased matrix stiffness promote the cardiac myofibroblast transition in 3D collagen matrices.," *Cardiovasc. Pathol.*, vol. 20, no. 6, pp. 325–33, 2011.

[69] B. N. Mason, J. P. Califano, and C. A. Reinhart-king, "Matrix Stiffness: A Regulator of Cellular Behavior and Tissue Formation," in *Engineering Biomaterials for Regenerative Medicine*, S. K. Bhatia, Ed. New York, NY: Springer New York, 2012, pp. 19–38.

[70] S. Kumar and V. M. Weaver, "Mechanics, malignancy, and metastasis: the force journey of a tumor cell.," *Cancer Metastasis Rev.*, vol. 28, no. 1–2, pp. 113–27, Jun. 2009.

[71] J. K. Mouw, Y. Yui, L. Damiano, R. O. Bainer, J. N. Lakins, I. Acerbi, G. Ou, A. C. Wijekoon, K. R. Levental, P. M. Gilbert, E. S. Hwang, Y.-Y. Chen, and V. M. Weaver, "Tissue mechanics modulate microRNA-dependent PTEN expression to regulate malignant progression.," *Nat. Med.*, vol. 20, no. 4, pp. 360–7, Apr. 2014.

[72] R. W. Tilghman, C. R. Cowan, J. D. Mih, Y. Koryakina, D. Gioeli, J. K. Slack-Davis, B. R. Blackman, D. J. Tschumperlin, and J. T. Parsons, "Matrix rigidity regulates cancer cell growth and cellular phenotype.," *PLoS One*, vol. 5, no. 9, p. e12905, Jan. 2010.

[73] R. W. Tilghman, E. M. Blais, C. R. Cowan, N. E. Sherman, P. R. Grigera, E. D. Jeffery, J. W. Fox, B. R. Blackman, D. J. Tschumperlin, J. a Papin, and J. T. Parsons, "Matrix rigidity regulates cancer cell growth by modulating cellular metabolism and protein synthesis.," *PLoS One*, vol. 7, no. 5, p. e37231, Jan. 2012.

[74] B. J. Gill, D. L. Gibbons, L. C. Roudsari, J. E. Saik, Z. H. Rizvi, J. D. Roybal, J. M. Kurie, and J. L. West, "A synthetic matrix with independently tunable biochemistry and

mechanical properties to study epithelial morphogenesis and EMT in a lung adenocarcinoma model.," *Cancer Res.*, vol. 72, no. 22, pp. 6013–23, Nov. 2012.

[75] K. Mi, G. Wang, Z. Liu, Z. Feng, B. Huang, and X. Zhao, "Influence of a self-assembling peptide, RADA16, compared with collagen I and Matrigel on the malignant phenotype of human breast-cancer cells in 3D cultures and in vivo.," *Macromol. Biosci.*, vol. 9, no. 5, pp. 437–43, May 2009.

[76] Y. Liang, J. Jeong, R. J. DeVolder, C. Cha, F. Wang, Y. W. Tong, and H. Kong, "A cell-instructive hydrogel to regulate malignancy of 3D tumor spheroids with matrix rigidity.," *Biomaterials*, vol. 32, no. 35, pp. 9308–15, Dec. 2011.

[77] D. Yip and C. H. Cho, "A multicellular 3D heterospheroid model of liver tumor and stromal cells in collagen gel for anti-cancer drug testing," *Biochem. Biophys. Res. Commun.*, vol. 433, pp. 327–332, 2013.

[78] Y. K. Girard, C. Wang, S. Ravi, M. C. Howell, J. Mallela, M. Alibrahim, R. Green, G. Hellermann, S. S. Mohapatra, and S. Mohapatra, "A 3D fibrous scaffold inducing tumoroids: a platform for anticancer drug development.," *PLoS One*, vol. 8, no. 10, p. e75345, Jan. 2013.

[79] J. N. Beck, A. Singh, A. R. Rothenberg, J. H. Elisseeff, and A. J. Ewald, "The independent roles of mechanical, structural and adhesion characteristics of 3D hydrogels on the regulation of cancer invasion and dissemination.," *Biomaterials*, vol. 34, no. 37, pp. 9486–95, Dec. 2013.

[80] F. Liu and D. J. Tschumperlin, "Micro-mechanical characterization of lung tissue using atomic force microscopy.," *J. Vis. Exp.*, no. 54, pp. 1–7, Jan. 2011.

[81] A. Majid, Y. Patil-Sen, W. Ahmed, and T. Sen, "Tunable Self-Assembled Peptide

Structure: A Novel Approach to Design Dual-Use Biological Agents," *Mater. Today Proc.*, vol. 4, no. 1, pp. 32–40, 2017.

[82] J. Ryu and C. B. Park, "High-temperature self-assembly of peptides into vertically well-aligned nanowires by aniline vapor," *Adv. Mater.*, vol. 20, no. 19, pp. 3754–3758, 2008.

[83] L. Adler- Abramovich, M. Reches, V. L. Sedman, S. Allen, S. J. B. Tendler, and E. Gazit, "Thermal and Chemical Stability of Diphenylalanine Peptide Nanotubes:Implications for Nanotechnological Applications," *Langmuir*, vol. 22, no. 20, p. 1313, 2006.

[84] M. Zhang, M. Yudasaka, A. Koshio, and S. Iijima, "Thermogravimetric analysis of single-wall carbon nanotubes ultrasonicated in monochlorobenzene," *Chem. Phys. Lett.*, vol. 364, no. 3–4, pp. 420–426, 2002.

[85] S. R. Shin, B. Aghaei-Ghareh-Bolagh, T. T. Dang, S. N. Topkaya, X. Gao, S. Y. Yang, S. M. Jung, J. H. Oh, M. R. Dokmeci, X. S. Tang, and A. Khademhosseini, "Cell-laden microengineered and mechanically tunable hybrid hydrogels of gelatin and graphene oxide.," *Adv. Mater.*, vol. 25, no. 44, pp. 6385–91, Nov. 2013.

[86] Y. Wang, W. C. Lee, K. K. Manga, P. K. Ang, J. Lu, Y. P. Liu, C. T. Lim, and K. P. Loh, "Fluorinated graphene for promoting neuro-induction of stem cells.," *Adv. Mater.*, vol. 24, no. 31, pp. 4285–90, Aug. 2012.

[87] M. R. Caplan, P. N. Moore, S. Zhang, R. D. Kamm, and D. a Lauffenburger, "Self-assembly of a beta-sheet protein governed by relief of electrostatic repulsion relative to van der Waals attraction.," *Biomacromolecules*, vol. 1, no. 4, pp. 627–31, Jan. 2000.

[88] A. Nagayasu, H. Yokoi, J. a Minaguchi, Y. Z. Hosaka, H. Ueda, and K. Takehana, "Efficacy of self-assembled hydrogels composed of positively or negatively charged peptides as scaffolds for cell culture.," *J. Biomater. Appl.*, vol. 26, no. 6, pp. 651–65, Feb.

2012.

List of Figures:

Figure 1. NIH-3T3 cells seeded and cultured on EFK8 hydrogel after (a) 1, (b) 3 and (c) 5 days of seeding and on EFK8-SWNT hybrid hydrogels after (d) 1, (e) 3 and (f) 5 days of seeding (scale bar: 400 μm). Confocal microscopy images of (g) EFK8 and (h) EFK8-SWNT at higher magnification (scale bar: 20 μm). Cells were stained for f-actin using Actin Green™ (green) and for nuclei with DAPI (blue)). (i) RADA16-I hydrogel disrupted one day after seeding the cells (scale bar: 1000 μm).

Figure 2. (a-b) NIH-3T3 cell colonies on EFK8 hydrogel at different magnifications. (c-f) Individually spread cells on the hybrid EFK8-SWNT hydrogel at different magnifications. Cell protrusions responsible for cell attachment to the scaffold are apparent in (f).

Figure 3. (a) NIH-3T3 cell proliferation on the EFK8 and EFK8-SWNT hydrogels incubated for one, three and five days after seeding. All data represent mean ± s.d. $*P < 0.05$. (b) Cell viability.

Figure 4. Optical (a) and confocal (b) microscopy images of an EFK8-SWNT hydrogel prepared within an EFK8 hydrogel. Z-stack images (c,d) obtained at different angles show the 3-dimensional structure of the cells within the hybrid hydrogel.

Figure 5. 3D cells after day one, three and five after encapsulation in EFK8 (a-c) and EFK8-SWNT (d-f) hydrogels, respectively.

Figure 6. (a) Compressive modulus of various hydrogels. (b) Optical image of NIH-3T3 cells after 5 days of seeding on EFK8 hydrogel formed from peptide at concentration 5 mg ml^{-1} (scale bar: 400 μm).

Figure 7. Optical images showing the evolution of A549 lung cancer cells seeded on different hydrogels from Day 4 to Day 12. **Left column**: Formation of spheroidal colonies of cancer cells induced by seeding on an EFK8 hydrogel formed from 1.25 mg ml^{-1} peptide. **Middle column:** Evidence of cancer cell movement after seeding on EFK8 hydrogel formed from 5 mg ml^{-1} peptide. **Right column:** Evidence of cancer cell movement after seeding on EFK8-SWNT hybrid hydrogel formed from 1.25 mg ml^{-1} peptide (scale bar: 200 μm).

Figure 8. Staining A549 lung cancer cells using Calcein AM on (a) EFK8 hydrogel and (b) EFK8 (5 mg ml^{-1}) hydrogel. In (a) green color of Calcein AM is replaced with a spectrum of different colors that represent different distances from the hydrogel surface. Immunostaining of A549 cells for β-catenin (green) and nucleus (blue) on (c) EFK8, (d) EFK8 (5 mg ml^{-1}) and (e) EFK8-SWNT hydrogels. Scale bar is 20 μm.

Statement of Significance

1- For the first time we used hybrid self-assembling peptide-carbon nanotube hybrid hydrogels (that we have recently introduced briefly in the "Carbon" journal in 2014) for tissue engineering and 3D tumor engineering.

2- We showed the potential of these hybrid hydrogels to enhance the efficiency of the peptide hydrogels for tissue engineering application in terms of cell behavior (cell attachment, spreading and migration). This opens up new rooms for the peptide hydrogels and can expand their applications.

3- Also our system (peptide and peptide-CNT hydrogels) was used for cancer cell spheroid formation showing the effect of both tumor microenvironment stiffness and cell-scaffold adhesion on cancer cell invasion. This was only possible based on the presence of CNTs in the hydrogel while the stiffness kept constant.

4- Finally it should be noted that these hybrid hydrogels expand applications of peptide hydrogels through enhancing their capabilities and/or adding new properties to them.

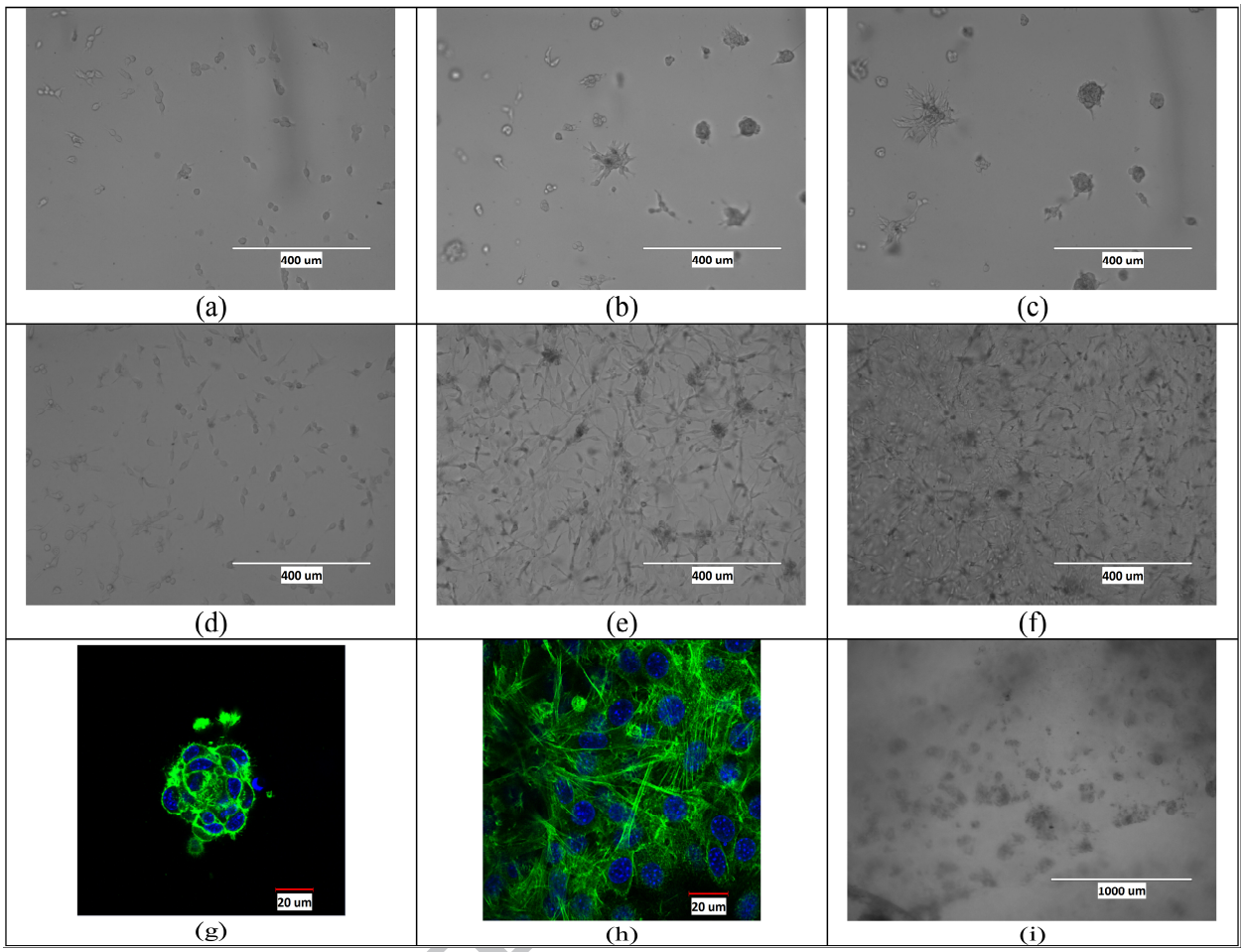

(a) (b) (c)

(d) (e) (f)

(g) (h) (i)

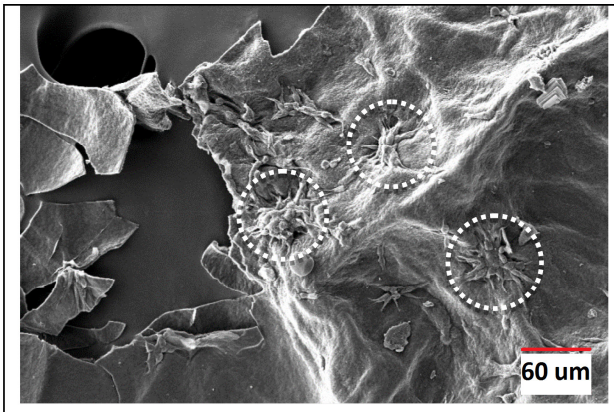

(a)

(b)

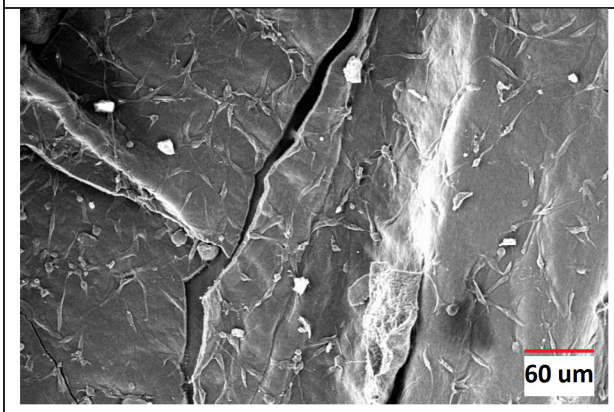

(c)

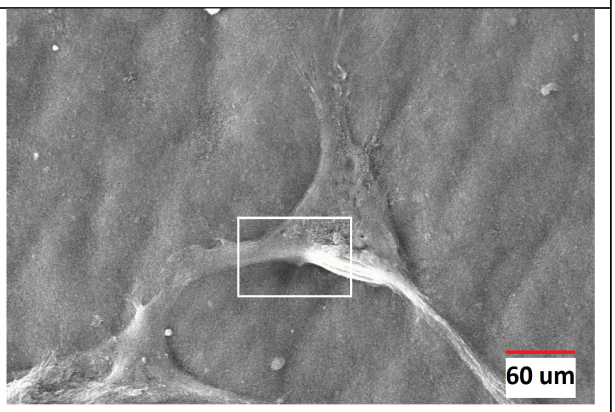

(d)

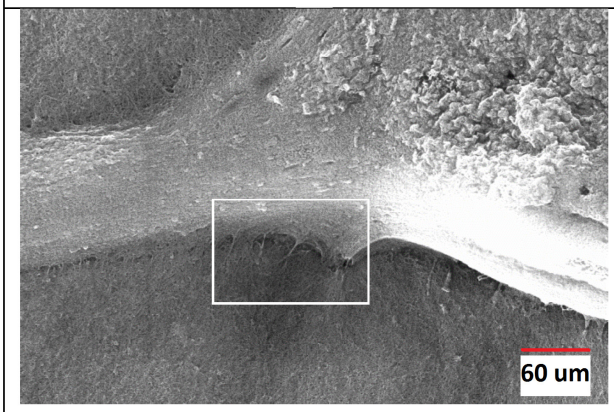

(e)

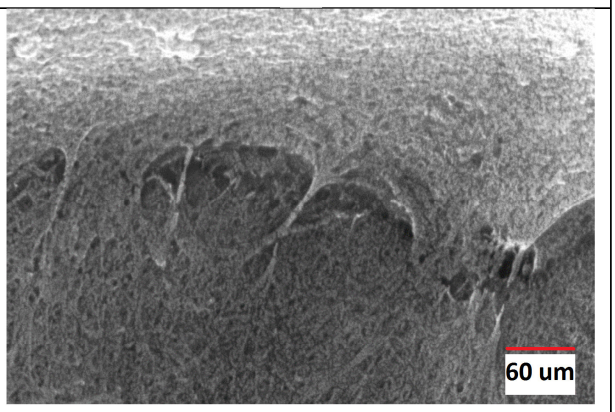

(f)

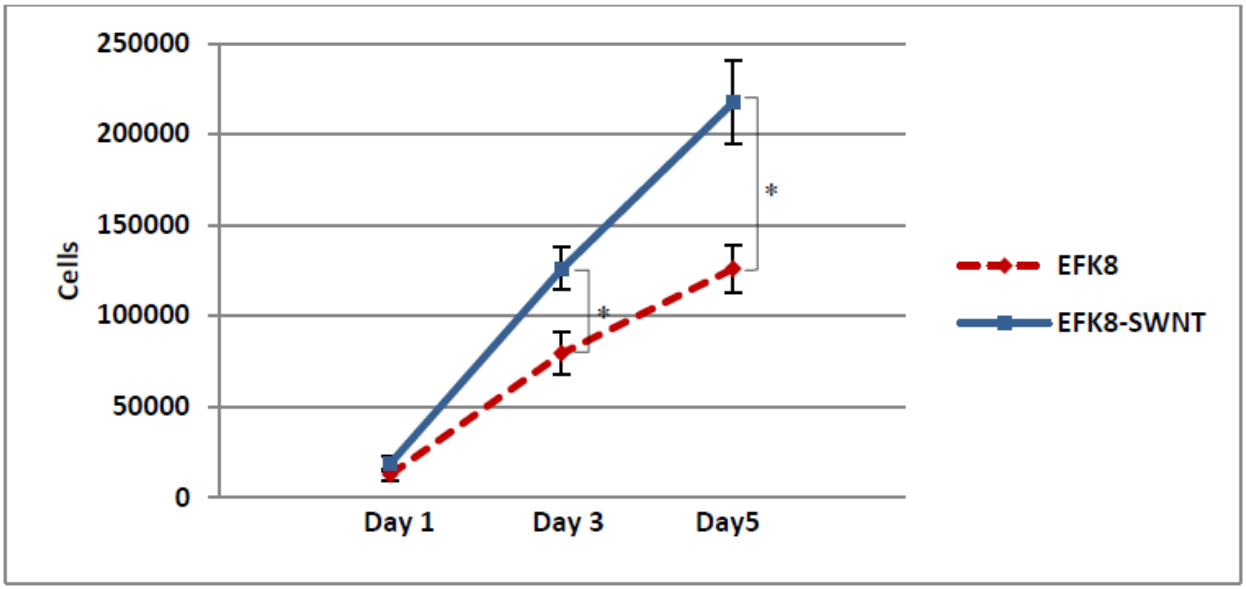

(a)

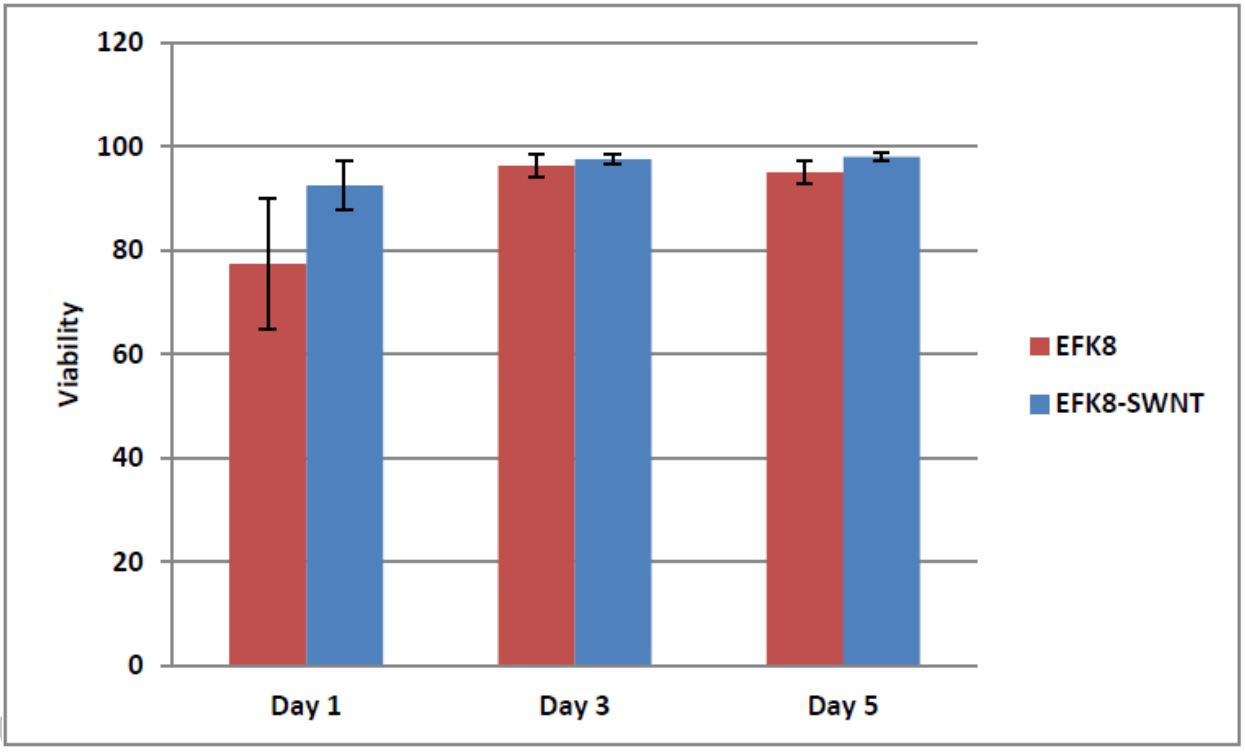

(b)

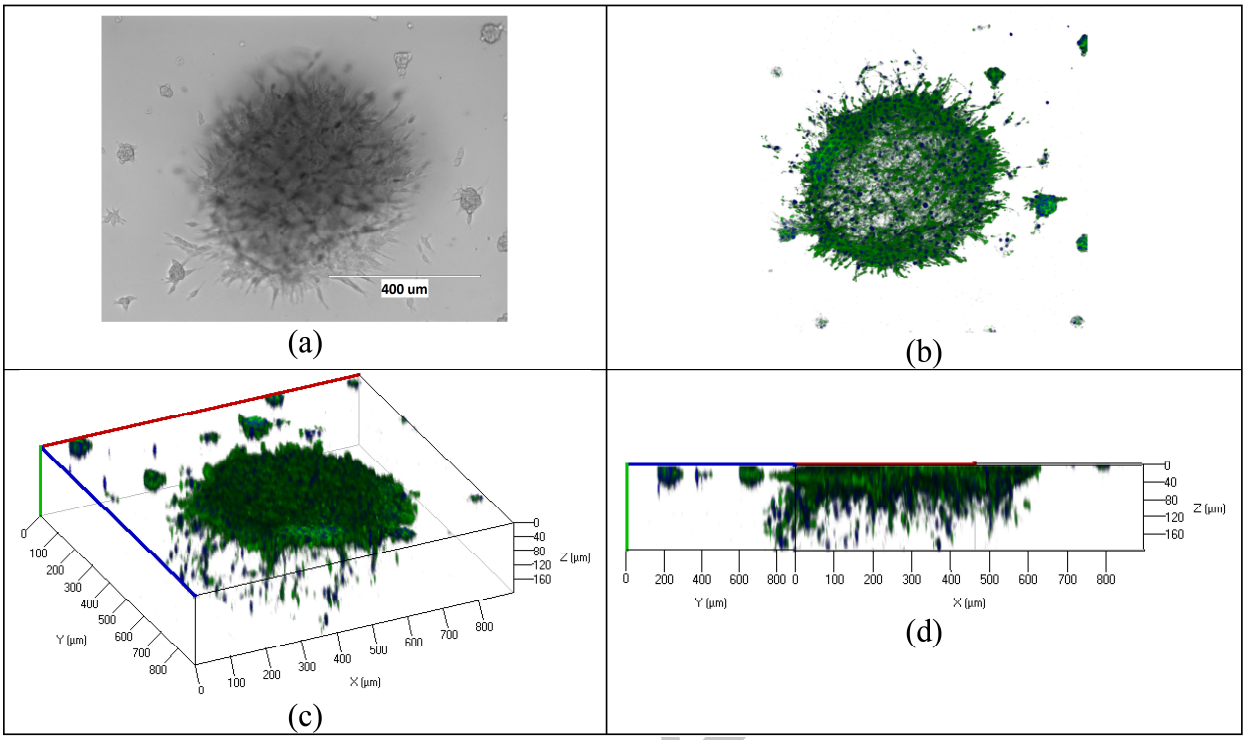

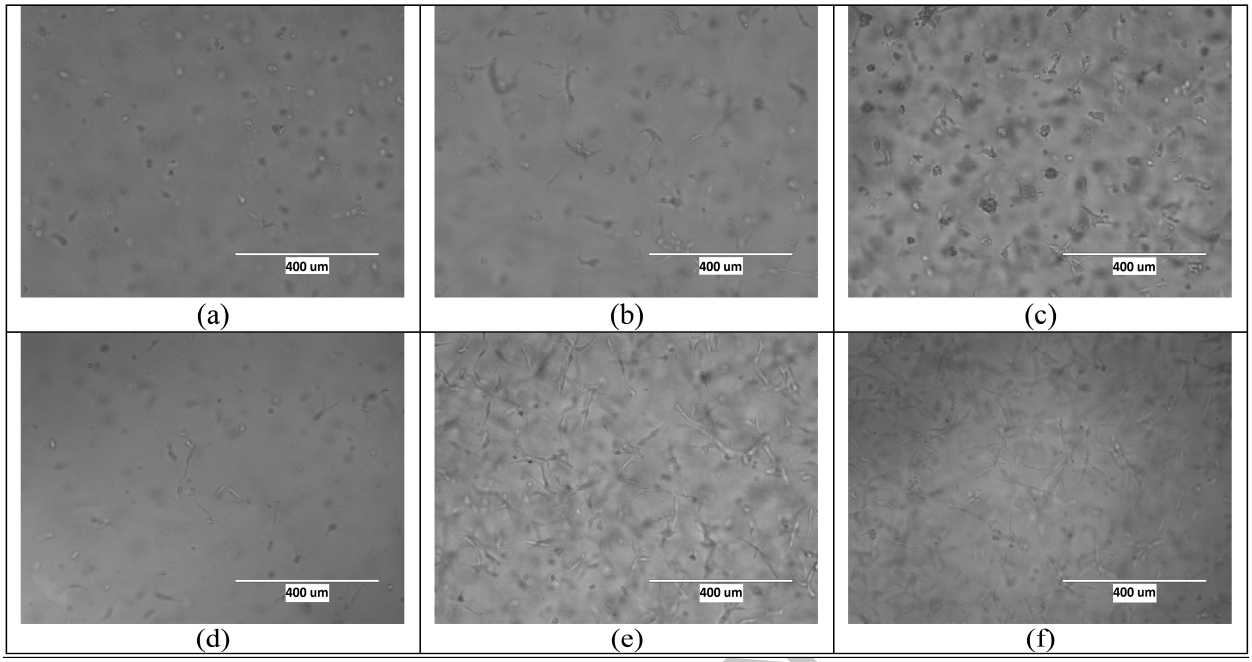

(a) (b) (c)

(d) (e) (f)

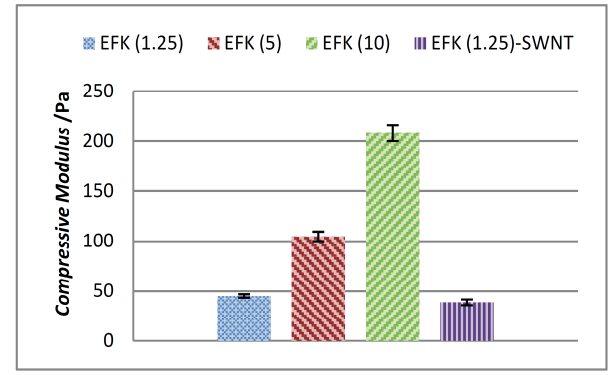

(a)

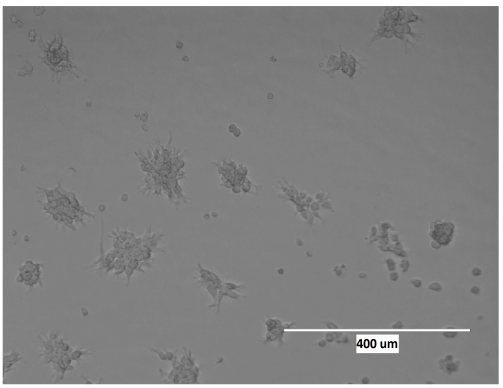

(b)

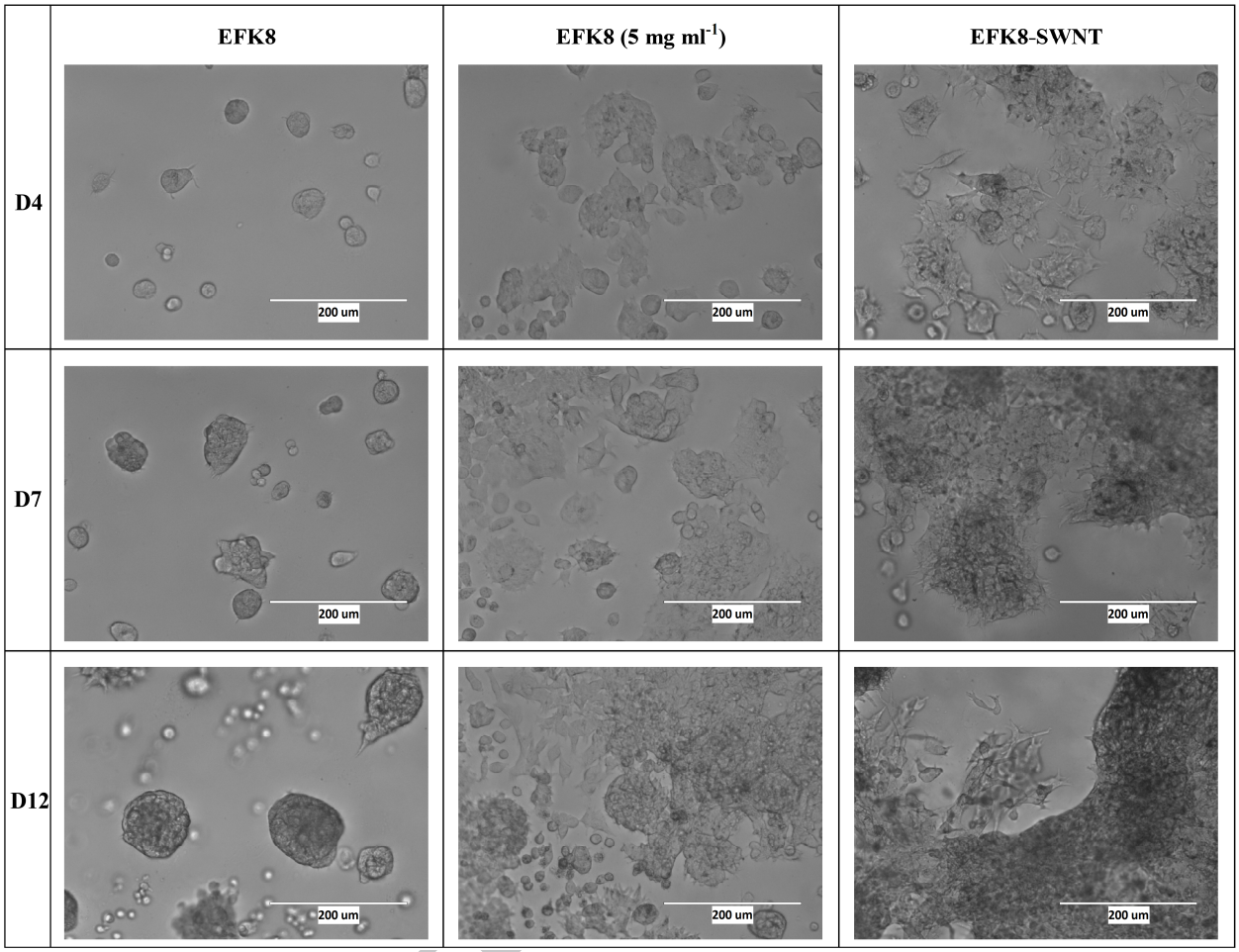

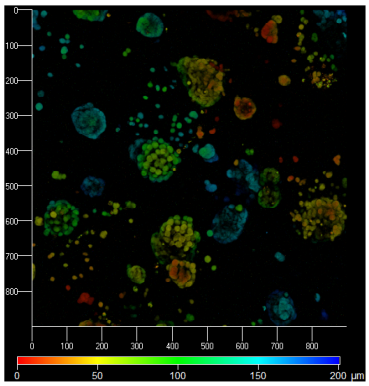

(a)

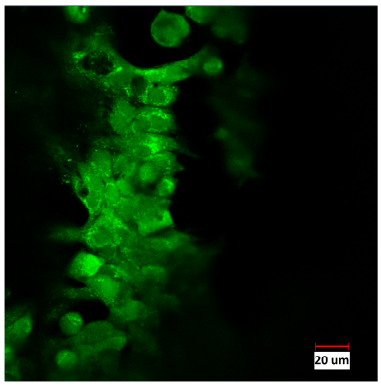

(b)

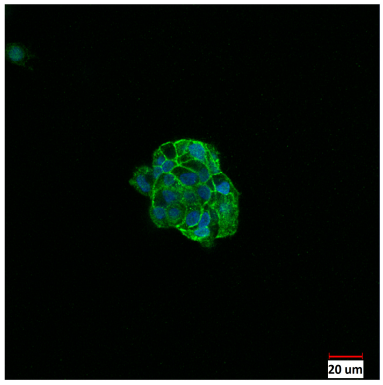

(c)

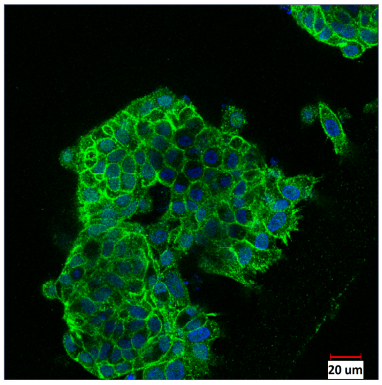

(d)

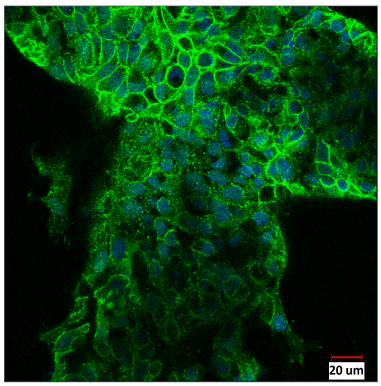

(e)

Effect of Presence of SWNTs in the Peptide Hydrogel on the Cell Behavior